



Distinct branches of the N-end rule pathway modulate the plant immune response

Jorge Vicente¹, Guillermina M. Mendiondo¹, Jarne Pauwels^{2,3}, Victoria Pastor⁴, Yovanny Izquierdo⁵, Christin Naumann^{6,7}, Mahsa Movahedi⁸, Daniel Rooney¹, Daniel J. Gibbs¹, Katherine Smart⁹, Andreas Bachmair¹⁰, Julie E. Gray⁸, Nico Dissmeyer^{6,7} , Carmen Castresana⁵, Rumiana V. Ray¹, Kris Gevaert^{2,3} and Michael J. Holdsworth¹ 

¹School of Biosciences, University of Nottingham, Nottingham, LE12 5RD, UK; ²VIB-UGent Center for Medical Biotechnology, Albert Baertsoenkaai 3, B-9000 Ghent, Belgium; ³Department of Biochemistry, Ghent University, Albert Baertsoenkaai 3, B-9000 Ghent, Belgium; ⁴Área de Fisiología Vegetal, Departamento de Ciencias Agrarias y del Medio Natural, Universitat Jaume I, Castellón E-12071, Spain; ⁵Centro Nacional de Biotecnología CSIC, C/Darwin, 3, Campus of Cantoblanco, E-28049 Madrid, Spain; ⁶Leibniz Institute of Plant Biochemistry (IPB), Weinberg 3, D-06120 Halle (Saale), Germany; ⁷Science Campus Halle – Plant-Based Bioeconomy, 06120 Halle (Saale), Germany; ⁸Department of Molecular Biology and Biotechnology, University of Sheffield, Sheffield, S10 2TN, UK; ⁹SABMiller Plc, SABMiller House, Church Street West, Woking, GU21 6HS, UK; ¹⁰Department of Biochemistry and Cell Biology, Max F. Perutz Laboratories, University of Vienna, Dr. Bohr Gasse 9, Vienna A-1030, Austria

Summary

Authors for correspondence:

Michael J. Holdsworth

Tel: +44 1159516046

Email:

michael.holdsworth@nottingham.ac.uk

Jorge Vicente

Tel: +44 1159516046

Email:

Jorge.Vicente_Conde@nottingham.ac.uk

Received: 18 May 2018

Accepted: 11 July 2018

New Phytologist (2019) 221: 988–1000

doi: 10.1111/nph.15387

Key words: amino-terminal glutamine amidase, Group VII Ethylene Response Factor transcription factor, N-end rule pathway, plant immunity, proteostasis.

- The N-end rule pathway is a highly conserved constituent of the ubiquitin proteasome system, yet little is known about its biological roles.
- Here we explored the role of the N-end rule pathway in the plant immune response. We investigated the genetic influences of components of the pathway and known protein substrates on physiological, biochemical and metabolic responses to pathogen infection.
- We show that the glutamine (Gln) deamidation and cysteine (Cys) oxidation branches are both components of the plant immune system, through the E3 ligase PROTEOLYSIS (PRT)6. In *Arabidopsis thaliana* Gln-specific amino-terminal (Nt)-amidase (NTAQ1) controls the expression of specific defence-response genes, activates the synthesis pathway for the phytoalexin camalexin and influences basal resistance to the hemibiotroph pathogen *Pseudomonas syringae* pv *tomato* (*Pst*). The Nt-Cys ETHYLENE RESPONSE FACTOR VII transcription factor substrates enhance pathogen-induced stomatal closure. Transgenic barley with reduced *HvPRT6* expression showed enhanced resistance to *Ps. japonica* and *Blumeria graminis* f. sp. *hordei*, indicating a conserved role of the pathway.
- We propose that that separate branches of the N-end rule pathway act as distinct components of the plant immune response in flowering plants.

Introduction

The regulation of protein stability through the ubiquitin proteasome system (UPS) is a central component of cellular homeostasis, environment interactions and developmental programmes (Varshavsky, 2012), and an important component of the plant immune system (Zhou & Zeng, 2017). Plants have evolved to recognize the presence of a pathogen in two main ways. Basal (primary) defence is characterised by the recognition of pathogen elicitors called pathogen associated molecular patterns (PAMPs) by protein receptors known as pattern recognition receptors (PRR), activating PAMP-triggered immunity (PTI) (Boller & Felix, 2009). When this response is effective, pathogens can deliver effector molecules into the host cells to weaken PTI and facilitate infection triggering a second layer of defence (effector triggered immunity; ETI). ETI is typically a qualitative response

based on interference with pathogen effector activity by plant resistance (R) gene products, localized inside the cell (Dangl & Jones, 2001). Both PTI and ETI induce similar immune responses but of different amplitude, with ETI often resulting in a hypersensitive response (HR). The specific set of mechanisms activated also depend to a large extent on the life strategy of the pathogen and how adapted they are to the host. Typically, the plant hormones jasmonic acid (JA) and ethylene (ET) mediate responses to nonadapted necrotrophs that cause host cell death to acquire nutrients from dead or senescent tissues (Grant & Jones, 2009; Pieterse *et al.*, 2009) whilst salicylic acid (SA) plays a crucial role in activating defence against adapted biotrophs and hemibiotrophs. Recently, regulation of protein stability by the Arg/N-end rule pathway of ubiquitin-mediated proteolysis has been demonstrated to play a role in plant responses to biotic stress. The pathway is associated with increased development of

clubroot caused by the obligate biotroph *Plasmodiophora brassicae* (Gravot *et al.*, 2016). Induction of components of the hypoxia response, controlled by Group VII ETHYLENE RESPONSE FACTOR (ERFVII) transcription factor substrates (ERFVIIIs), enhanced clubroot development, indicating that the protist hijacks the N-end rule ERFVII regulation system to enhance infection. In another study, inactivation of different components of the Arg/N-end rule pathway was shown to result in greater susceptibility of Arabidopsis to necrotrophic pathogens and altered timing and amplitude of response to the hemibiotroph *Pseudomonas syringae* pathovar *tomato* (*Pst*) AvrRpm1 (de Marchi *et al.*, 2016). A correlation between Nt-Acetylation and the stability of a Nod-like receptor, Suppressor of NPR1, Constitutive 1 (SNC1) was also reported (Xu *et al.*, 2015). Whilst these reports provide evidence that the N-end rule pathway is involved in the regulation of plant defence responses, the mechanisms, substrates or their function in resistance have not been investigated previously (Gibbs *et al.*, 2014a). The N-end rule pathway of ubiquitin-mediated proteolysis is an ancient and conserved branch of the UPS (Gibbs *et al.*, 2014a). This pathway relates the half-life of substrates to the amino-terminal (Nt-) residue, which forms part of an N-degron (Gibbs *et al.*, 2014a). Destabilizing residues of the Arg/N-end rule are produced following endo-peptidase cleavage and may be primary, secondary or tertiary (Fig. 1a). Basic and hydrophobic primary destabilizing residues are recognized directly by N-recognin E3 ligases, in plants represented by two proteins, PROTEOLYSIS(PRT)6 and PRT1 (Gibbs *et al.*, 2014a). Secondary destabilizing residues (Glu, Asp and oxidized Cys) can be N-terminally arginylated by arginyl-transferases (ATEs), and tertiary destabilizing residues (Gln, Asn and Cys) can undergo modifications to form secondary destabilizing residues (Gibbs *et al.*, 2014a). Oxidation of Cys was shown *in vitro* to occur both nonenzymically (Hu *et al.*, 2005) or enzymatically (Weits *et al.*, 2014; White *et al.*, 2017), whereas in higher eukaryotes deamidations of Gln and Asn are carried out by residue-specific N-terminal amidases (NTAQ1 (Wang *et al.*, 2009) and NTAN1 (Grigoryev *et al.*, 1996), respectively). This hierarchical structure is conserved in eukaryotes, and physiological substrates with N-terminal residues representing these destabilizing classes have been identified (Piatkov *et al.*, 2014). The Usp1 deubiquitylase is targeted for degradation through the deamidation branch of the Arg/N-end rule via NTAQ1 as a consequence of auto-cleavage, that reveals N-terminal Gln (Piatkov *et al.*, 2012). Proteins with similarities to mouse NTAN1 and NTAQ1 are encoded in higher plant genomes, in Arabidopsis by AT2G44420 (putative NTAN1) and AT2G41760 (putative NTAQ1). Expression of these in a deamidation deficient *nta1* mutant of *Saccharomyces cerevisiae* could functionally restore degradation of the N-end rule reporters Asn- β -galactosidase (β -Gal) and Gln- β -Gal, respectively. ATE activity was required for this destabilization in yeast (Graciet *et al.*, 2010). Although the Arg/N-end rule pathway is evolutionarily highly conserved in eukaryotes, few substrates or functions for different branches have been shown. In plants the Cys branch of the Arg/N-end rule pathway controls homeostatic response to hypoxia (low oxygen) and NO sensing through the Met-Cys initiating ERFVII

transcription factor substrates (Gibbs *et al.*, 2011, 2014b; Licausi *et al.*, 2011).

In this paper, we investigated the role of distinct branches of the Arg/N-end rule pathway in the immune response in Arabidopsis and barley (*Hordeum vulgare*). We demonstrate that two branches of the pathway, Glu-deamidation and Cys-oxidation, regulate resistance to the hemibiotroph *Pst* and the biotroph *Blumeria graminis* f. sp. *hordei* (*Bgh*). We also show a significant role for Nt-Gln amidase NTAQ1 in the regulation of molecular components associated with basal responses to infection, and a role for both NTAQ1 and the known Nt-Cys ERFVII substrates in resistance related to stomatal function.

Materials and Methods

Plant material, growth conditions and experimental design

Arabidopsis thaliana seeds were obtained from NASC, UK unless otherwise stated, including *prt6-1* (SAIL 1278_H11), *ntaq1-1* (SALK_075466). Mutant *ntan1-1* (Q202* mutation (CAA to TAA)) was obtained from the Seattle TILLING project (<http://tilling.fhcrc.org>). Mutant *ntaq1-3* was obtained from the GABI-Kat T-DNA insertion collection (GK_306F08). The *pad3-1* null allele was described previously (Glazebrook & Ausubel, 1994). Mutants are in the Col-0 (wild type, WT) accession. Plants were grown and assays performed in controlled-environment rooms under the following conditions: 12 h of light (23°C) and 12 h of dark (18°C), 60–70% relative humidity. Plants were treated between 3 and 4 wk after germination. Barley plant genotypes and growth conditions were as previously described (Mendiondo *et al.*, 2016).

Construction of transgenic Arabidopsis lines ectopically expressing NTAQ1

To generate Arabidopsis NTAQ1 overexpressing lines, full-length cDNA sequence (with and without the STOP codon) was amplified from 7-d-old seedling cDNA and recombined into pDONR221. The constructs were mobilized into pH7m34G and pH7m24GW2, with the GSrhino tag in C-terminal or N-terminal position of the NTAQ1, respectively (Karimi *et al.*, 2007). Then the constructs were transformed into *Agrobacterium tumefaciens* (strain GV3101 pMP90) and Arabidopsis *ntaq1-3* using standard protocols (Clough & Bent, 1998).

In vitro assay for NTAQ1 activity

The Arabidopsis NTAQ1 coding sequence was cloned from cDNA and flanked by an N-terminal tobacco etch virus (TEV) protease recognition sequence (ENLYFQ-X) using primers *ss_ntaq1_tev* and *as_ntaq1_gw*, followed by a second PCR with *as_ntaq1_gw* and adapter *tev* attaching a Gateway attB1 site for sub-cloning into pDONR201 (Invitrogen). An LR reaction into pVP16 (Thao *et al.*, 2005) leads to an N-terminal 8xHis:MBP double affinity tag. An assay for NTAQ activity was performed as described previously (Wang *et al.*, 2009) with slight modifications. The assay was performed in three technical replicates from three

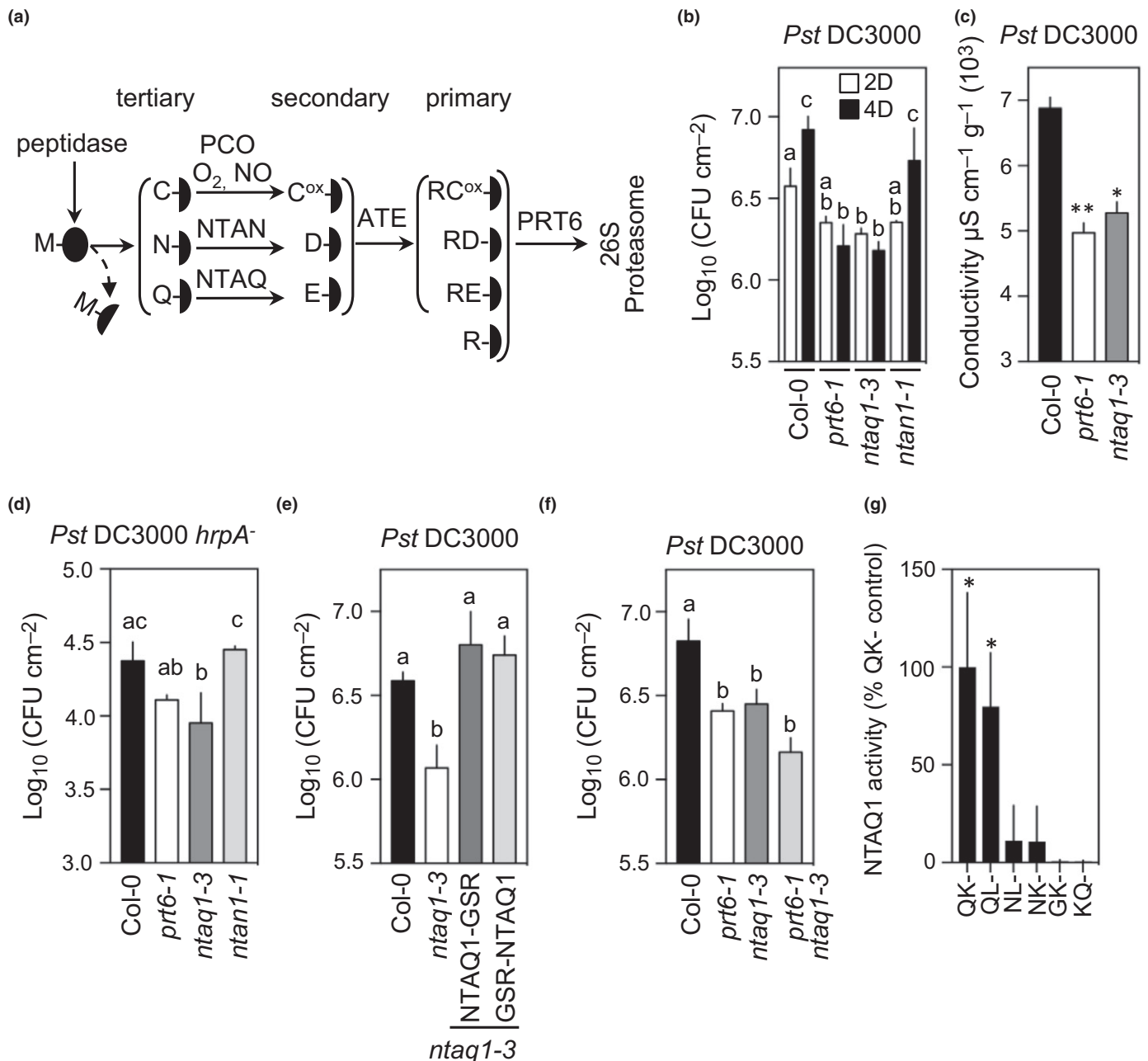


Fig. 1 Genetic characterization of the role of the N-end rule pathway in the Arabidopsis apoplastic response to *Pst* DC3000. (a) Schematic of the Arg/N-end rule pathway. Single letter codes for residues are shown. PRT6, PROTEOLYSIS6; ATE, arginyl transferase; NTAN, Nt-Asn amidase; NTAQ, Nt-Gln amidase; PCO, PLANT CYSTEINE OXIDASE. Black ovals represent protein substrates. (b) Quantification of *Pst* DC3000 growth in wild-type (WT) and mutant plants 2 d and 4 d after bacterial infiltration (10^6 colony forming units (CFU) ml^{-1}). (c) Ion leakage measurement in leaves 4 d after infiltration with *Pst* DC3000 (10^7 CFU ml^{-1}). (d–f) Quantification of bacterial growth in WT and mutant plants 4 d after bacterial infiltration (10^6 CFU ml^{-1}). (g) Enzyme activity of bacterially produced NTAQ1 against peptides with different Nt residues (– = GAGSW). Data represent means \pm SEM. Statistical differences were analyzed by ANOVA followed by Tukey test ($P < 0.05$), significant differences are indicated with letters, or Student's *t*-test: *, $P < 0.05$; **, $P < 0.01$.

independent NTAQ1 protein expressions. The activity of NTAQ1 towards QKGSAGW was used as the 100% reference value.

Analysis of pathogen growth in plant material

The bacterial suspension was injected with a needleless syringe into the abaxial side of leaves or sprayed on the surface of the

leaves of 3.5-wk-old plants. *Pst* DC3000 *avrRpm1*, *Pst* DC3000 and *Pst* DC3000 *hrpA*⁻ were grown overnight at 28°C in Petri dishes on King's B medium. For analysis of bacterial growth, three leaves per plant of at least seven plants were injected with a bacterial suspension of 10^6 CFU ml^{-1} ($\text{OD}_{600\text{ nm}} 0.1 = 10^8$ CFU ml^{-1}) or sprayed with a suspension of 10^8 CFU ml^{-1} . A disc of 0.28 cm^2 from each infected leaf was

excised at 96 h, pooled in triplicate, homogenized, diluted and plated for counting. Inoculation of *Botrytis cinerea* was performed by pipetting a drop of 10 μ l of a suspension of 5×10^5 spores ml^{-1} onto the surface of the leaves. The response was analyzed by measuring the diameter of the symptoms produced in three leaves of at least 20 independent plants.

Barley plants were infected with *Fusarium* spp. and *Blumeria graminis* f. sp. *hordei* as previously described (Ajigboye *et al.*, 2016). Leaf material of 25-d-old barley plants grown under controlled conditions (20°C:15°C; 16-h photoperiod; 80% RH, 500 $\mu\text{mol m}^{-2} \text{s}^{-1}$ metal halide lamps (HQI) and supplemented with tungsten bulbs) were syringe infiltrated with 0.1 OD *Ps. pv japonica* obtained from the National Collection of Plant Pathogenic Bacteria (NCPPB), UK. Leaf material was collected before treatment and 4 d after inoculation for conductivity assays and RNA extraction. Production of H_2O_2 was visualized by staining with 3,3'-diaminobenzidine tetrachloride as described (Thordal-Christensen *et al.*, 1997; Moreno *et al.*, 2005).

Stomatal aperture analyses

For stomatal aperture in response to *Pst* assays, leaves from 3.5-wk-old plants were used. In the morning after 2 h the lights were switched on and peels from the abaxial side of the leaves were placed in Petri dishes containing 10 mM MES/KOH pH 6.1, 50 mM KCl and 0.1 mM CaCl_2 for 2 h in continuous light. Then the buffer was replaced with a solution of *Pst* DC3000 (OD 0.2: 2×10^8 CFU ml^{-1}). Stomatal aperture was measured after 0, 1 and 3 h of incubation with the bacteria. Stomatal aperture measurements for ABA sensitivity assays were carried out on detached leaf epidermis as described previously (McAinsh *et al.*, 1991; Chater *et al.*, 2011).

Protein extraction and Immunoblotting

Protein extractions and immunoblotting were carried out as described previously (Gibbs *et al.*, 2011).

Gene expression analysis

RNA extraction, cDNA synthesis, semiquantitative and quantitative RT-PCR were performed as previously described for Arabidopsis (Gibbs *et al.*, 2011, 2014b) and barley (Mendondo *et al.*, 2016). For primers used see Supporting Information Table S1.

Analysis of nitrate reductase activity

Nitrate reductase was assayed as previously (Vicente *et al.*, 2017) with modifications described elsewhere (Kaiser & Lewis, 1984).

Analysis of protein, RNA and metabolites

Protein extraction, immunoblotting and histochemistry were carried out as described previously (Gibbs *et al.*, 2011). Quantitative RT-PCR was performed as previously described for Arabidopsis

(Gibbs *et al.*, 2014b) and barley (Mendondo *et al.*, 2016). Proteomics (Vu *et al.*, 2016) and metabolomics (Gamir *et al.*, 2012; Sánchez-Bel *et al.*, 2018) analyses were carried out as previously described.

Experimental statistical analyses

All experiments were performed at least in triplicate. Statistical comparisons were conducted using GraphPad PRISM 7.0 software. Horizontal lines represent standard error of the mean values in all graphs. For statistical comparisons we used Student's *t*-test, where statistically significant differences are reported as: ***, $P < 0.001$; **, $P < 0.01$; *, $P < 0.05$; and one-way analysis of variance (ANOVA) with Tukey's multiple comparisons test, where significant differences ($\alpha < 0.05$) are denoted with different letters.

Results

Nt-Gln amidase and Cys oxidation branches of the Arg/N-end rule pathway increase basal resistance against *Pst* DC3000

The role for the Arg/N-end rule pathway in the plant immune response was assessed using the model bacterial pathogen *P. syringae* pv *tomato* DC3000 and T-DNA insertion null mutants of the putative Gln-specific amino-terminal amidase NTAQ1 (AT2G41760) (Fig. S1a–d) and N-recogin E3 ligase PRT6 (AT5G02310) genes, and a premature termination allele of the putative Asn-specific amino-terminal amidase NTAN1 (AT2G44420) (Q202*) (Fig. 1a). The entire effect of NTAQ1, NTAN1 and Cys branches of the Arg/N-end rule pathway on response to pathogen challenge can be assessed by analysis of the *prt6* mutant, as this removes E3 ligase activity, thus stabilizing all substrates of NTAQ1, NTAN1 and substrates with Nt-Cys (Fig. 1a). Bacterial growth in leaves of *prt6* was significantly lower by 4 d post-infiltration with virulent (*Pst* DC3000) or avirulent (*Pst* DC3000 *avrRmp1*) strains, indicating that substrates destabilized by PRT6 action contribute to the immune response (Figs 1b, S2a). In comparison, *ntaq1* alleles also showed significantly lower bacterial growth (comparable with that of *prt6*) compared with both the *ntan1-1* mutant or the wild type (WT) Col-0 for plants grown from seed in soil under neutral days (12 h:12 h, light:dark). These results are opposite to those obtained by de Marchi *et al.* (2016), who found enhanced sensitivity to *Pst* DC3000 of N-end rule mutants *prt6* and *ate1 ate2* (which removes ATE Nt-arginylation activity, Fig. 1a). To investigate this difference, we assayed bacterial growth under conditions used by de Marchi *et al.* for plant growth and infection. In their case, germination and initial 7 d growth of seedlings was carried out on agar containing MS medium and 0.5% sucrose before transfer to soil and, following transfer, plants were grown under short-day conditions (9 h:15 h, light:dark). We grew Col-0, *prt6-1* and *ate1 ate2* under these conditions and assayed bacterial growth at 2 d and 4 d post-infiltration. For plants grown under neutral days, we found that by 4 d post-infection, bacterial growth was significantly lower in N-end rule mutants than in the

WT (Fig. S2b). All subsequent reported experiments were carried out using plants grown from seed under neutral-day conditions.

Tissue cellular leakage measured 4 d following infection was significantly lower in *prt6* and *ntaq1* mutants (Figs 1c, S1d). Expression in WT of *NTAQ1* and *PRT6* was not strongly affected by infection with either bacterial strain (Fig. S2c). Inoculation with the PTI inducer *Pst* DC3000 *hrpA*⁻ (with a compromised type-three secretion system), resulted in reduced susceptibility of *prt6* and *ntaq1* mutants compared with WT or *ntan1* (Fig. 1d). Ectopic expression of either Nt- or C-terminally tagged *NTAQ1* removed enhanced resistance of *ntaq1-3* (Fig. 1e), and the double mutant *prt6-1 ntaq1-3* did not show significant difference compared with the single mutants *prt6-1* or

ntaq1-3 (Fig. 1f). It was previously suggested that formation of N-terminal pyroglutamate by glutaminyl cyclase (GC) might compete with *NTAQ1* for Nt-Gln substrates (Wang *et al.*, 2009), implying that a lack of GC activity could lead to enhanced susceptibility. We observed a similar response to *Pst* DC3000 of WT and a mutant of *GLUTAMINYL CYCLASE1* (*GCI*) (Schilling *et al.*, 2007) (Fig. S2d), indicating that competition for Nt-Gln substrates between *NTAQ1* and *GCI* is not relevant for the regulation of bacterial growth following infection. To define the biochemical action of *NTAQ1*, we analysed the Nt-deamidation capacity of recombinant Arabidopsis *NTAQ1* that showed high specificity for Nt-Gln in comparison with Nt-Asn, -Gly and -Lys (Fig. 1g).

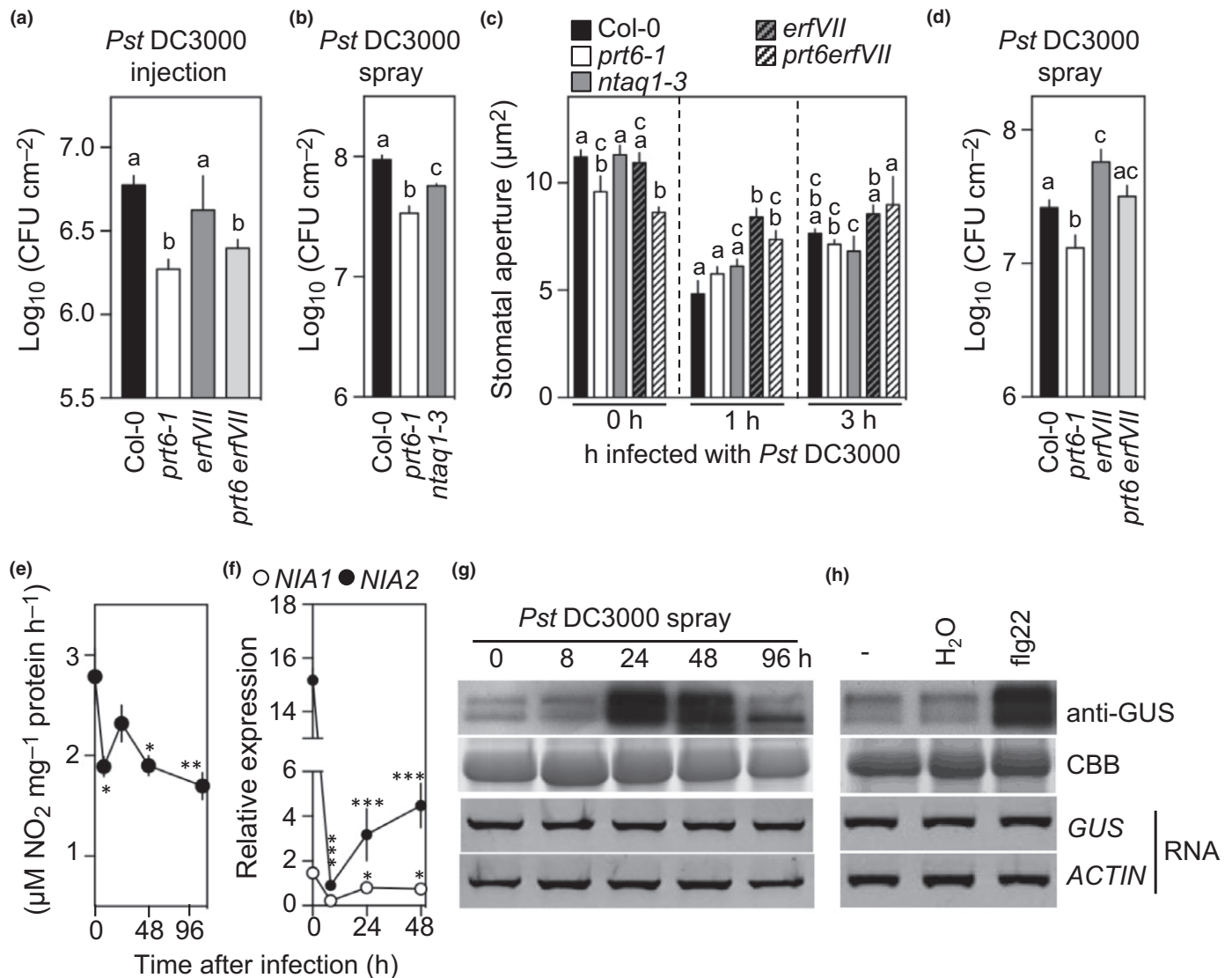


Fig. 2 Genetic characterization of the role of the N-end rule pathway in the Arabidopsis stomatal response to *Pst* DC3000. (a–d) Quantification of *Pst* DC3000 growth in wild type (WT) and mutant plants 4 d after bacterial infiltration by injection (10^6 colony forming units (CFU) ml^{-1}) or bacterial foliar spray application (10^8 CFU ml^{-1}). (c) Stomatal aperture response to applied *Pst* DC3000 in WT and mutants. (e) Total NR enzyme activity following foliar application of *Pst* DC3000 (10^8 CFU ml^{-1}). (f) Expression of *NIA1* and *NIA2* RNA following leaf infiltration with *Pst* DC3000. (g) Stabilisation of C-HA GUS protein and expression of *MC-HA GUS* and *ACTIN* RNA in WT Arabidopsis plants sprayed with *Pst* DC3000 (10^8 CFU ml^{-1}). (h) Stabilisation of C-HA GUS 24 h after injection with flg22 (1 μM) or H₂O. CBB, Coomassie Brilliant Blue. Data represent means \pm SEM. Statistical differences were analyzed by ANOVA followed by Tukey test ($P < 0.05$), significant differences are indicated with letters, or Student's *t*-test: *, $P < 0.05$; **, $P < 0.01$; ***, $P < 0.001$.

Using mutants in which ERFVII activity was removed (Abbas *et al.*, 2015) (*rap2.12 rap2.2 rap2.3 bre1 bre2* pentuple mutant, hereafter *erfVII*, and the *prt6 erfVII* sextuple mutant), analysis of infections of *Pst* DC3000 following infiltration showed no significant influence of ERFVII in affecting apoplastic growth of either virulent or avirulent *Pst* strains (Figs 2a, S3a). Bacterial growth 4 d following foliar spray application of *Pst* DC3000 revealed greater resistance of both *prt6-1* and *ntaq1-3* mutants compared with WT or *ntan1-1* (Figs 2b, S3b), which for both foliar spray and injection required SA, analysed in double mutant combinations of *prt6-1* or *ntaq1-3* with *sid2-1*. SID2 is an isochorismate synthase required for SA synthesis (Nawrath & Metraux, 1999) (Fig. S3c). Stomatal closure is a key component of early defence response following pathogen attack (Arnaud & Hwang, 2015). We found that, in response to *Pst*, WT initially closed and then, induced by the pathogen, reopened its stomata, as did *prt6-1* and *ntaq1-3*. The *erfVII* and *prt6 erfVII* mutants failed to close stomata at any point (Fig. 2c). ERFVII have previously been shown to regulate stomatal ABA sensitivity via the N-end rule pathway (Vicente *et al.*, 2017), and we also found *ntaq1-3* stomata were hypersensitive to ABA (Fig. S3d). In response to *Pst* DC3000 infection following foliar spray application, resistance was significantly lower in the absence of ERFVII transcription factors (either *erfVII* or *prt6 erfVII*) compared with WT or *prt6* (Fig. 2d), respectively. Response to the foliar spray application of *Pst* DC3000 was associated with a large decrease in activity and expression of NITRATE REDUCTASE (NR) (Fig. 2e,f). This reduction has been previously linked with increased basal resistance against *Pst* (Park *et al.*, 2011), whereas expression of *ADH1*, a marker for hypoxia, was only increased immediately following pathogen challenge (Fig. S3e). Infection with *Pst* DC3000 was associated by 24 h with increased stabilization of an artificial Cys-Arg/N-end rule substrate derived from the construct *35S:MC^{HA}GUS*, that following constitutive MetAP activity is expressed as C-^{HA}GUS (Gibbs *et al.*, 2014b; Vicente *et al.*, 2017) (Fig. 2g). To clarify whether plant-derived factors were solely responsible for the control of the stability of C-^{HA}GUS, we injected the PAMP peptide *flg22*, and showed that injection of *flg22* was able to stabilize C-^{HA}GUS (Fig. 2h).

The Arg/N-end rule pathway has a conserved function in the immune response

To determine the conservation of Arg/N-end rule pathway role in the immune response, we tested responses to pathogens in barley, a monocot species distantly related to Arabidopsis, in which the expression of the *PRT6* orthologue gene *HvPRT6* was reduced by RNAi (Mendondo *et al.*, 2016). Following inoculation with a strain of *P. syringae* pv *japonica* with known pathogenicity to barley (Dey *et al.*, 2014), significantly lower bacterial load was observed in *HvPRT6* RNAi leaves compared with the WT (Fig. 3a). Similarly, *HvPRT6* RNAi plants exhibited reduced development and severity of mildew caused by *Bgh* (Fig. 3b,c). By contrast, susceptibility of *HvPRT6* RNAi to *Fusarium graminearum* or *F. culmorum*, tested on detached leaves was increased compared with the WT (Fig. 3d). To assess the

response of *prt6-1* in Arabidopsis to a necrotroph we inoculated the mutant and WT with the fungal pathogen *B. cinerea* but we failed to observe any significant differences in disease severity, measured as diameter of necrotic lesions (Fig. S3f). Infection of barley with *Ps* pv *japonica* or *Bgh* also resulted in accumulation of the artificial Nt-Cys substrate CCGAIL-GUS (from *pUBI: MCGGAIL-GUS*, containing the first highly conserved seven residues of ERFVII; Gibbs *et al.*, 2014b; Mendiondo *et al.*, 2016; Vicente *et al.*, 2017), therefore Nt-Cys stabilization in response to infection is conserved in flowering plants (Fig. 3e).

NTAQ1 regulates expression of the camalexin biosynthesis pathway

A shotgun proteomic analysis of total proteins from untreated *ntaq1-3* and WT adult leaves revealed 13 proteins which were significantly differentially regulated, 12 exhibited increased and one decreased abundance in *ntaq1-3* (Table S2). The functions of most *ntaq1* upregulated proteins are related to oxidative, biotic and abiotic stresses, including a 2-OXOGLUTARATE OXYGENASE (AT3G19010) potentially involved in quercetin biosynthesis and targeted by bacterial effectors (Truman *et al.*, 2006) and DJ-1 protein homolog E (DJ1E) involved in response to PAMPs (Lehmeyer *et al.*, 2016). Not all *ntaq1* upregulated proteins were also upregulated at the level of RNA (Fig. S4). Several *ntaq1* over-accumulated proteins are involved in the regulation of reactive oxygen species (ROS). However, analysis of gene expression of a ROS accumulation marker, the antioxidant enzyme CATALASE1 (CAT1), and histochemical analysis of the accumulation of the ROS hydrogen peroxide (H₂O₂) during infections with *Pst* failed to reveal significant differences between the mutants *ntaq1* and *prt6* and WT (Fig. S5). Increased tolerance of the mutants which was associated with less cellular damage required SID2, an isochorismate synthase required for SA synthesis (Nawrath & Metraux, 1999), as double mutant combinations of *prt6-1* or *ntaq1-3* with *sid2-1* showed susceptibility similar to the *sid2* single mutant (Fig. S3c). Analysis of phytohormone levels indicated that there were no differences between *ntaq1-3*, *prt6-1* or WT in untreated or infected leaves for SA, JA or IAA (Figs 4, S6). These results together suggest a functional redundancy of *ntaq1* upregulated proteins with other antioxidant mechanisms, already documented in the case of the GLUTATHIONE S-TRANSFERASEs (GSTs) (Sappl *et al.*, 2009), or alternative roles for *ntaq1* upregulated proteins in plant defence.

One of the identified proteins upregulated in *ntaq1*, the phi class GSTF6, functions in secondary metabolism related to the synthesis of the major Arabidopsis phytoalexin, camalexin (Su *et al.*, 2011), as do the upregulated proteins PUTATIVE ANTHRANILATE PHOSPHORIBOSYLTRANSFERASE (involved in the synthesis of the camalexin precursor tryptophan; Zhao & Last, 1996) and IAA-AMINO ACID HYDROLASE (ILL4), that generates indole-3-acetic acid (IAA) from its conjugated form (Davies *et al.*, 1999). Another upregulated protein, GSTF7 was hypothesized to play a role in camalexin synthesis based on its induction in the constitutively active MKK9 mutant

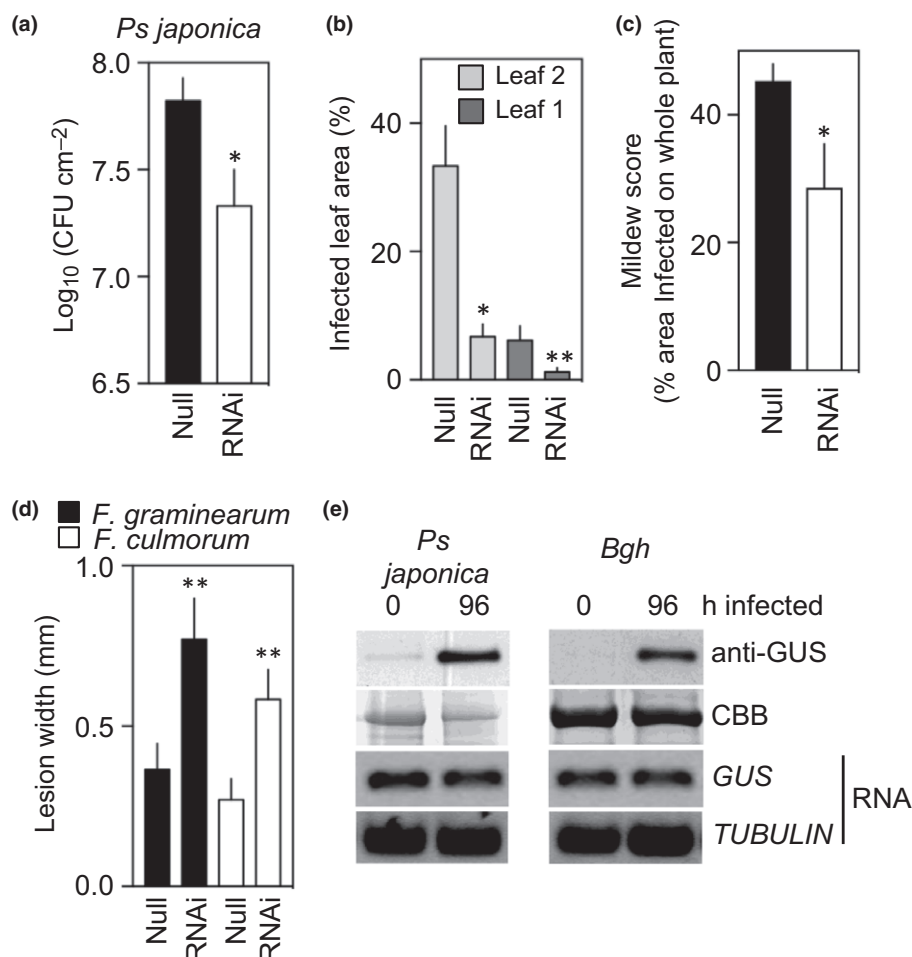


Fig. 3 Analysis of N-end rule function in barley. (a) Quantification of *Ps pv japonica* growth in *HvPRT6* RNAi and wild type (WT) (cv Golden Promise) (null segregant from the same transformation event) plants 4 d after bacterial infiltration (10^8 colony forming units (CFU) ml⁻¹). (b, c) Measurement of total and leaf area infected in WT and *HvPRT6* RNAi barley plants with *Blumeria graminis* f. sp. *hordei* (*Bgh*). (d) Necrotic lesions on WT and *HvPRT6* RNAi barley plants 5 d following inoculation with *Fusarium graminearum* or *F. culmorum*. (e) Stabilisation of CGGAIL-GUS and expression of MCGGAIL-GUS and *TUBULIN* RNA in barley following infection with *Ps pv japonica* (10^8 CFU ml⁻¹) (4 d) or *Bgh* (14 d). CBB, Coomassie Brilliant Blue. Data represent means \pm SEM. Statistical differences were analyzed Student's *t*-test: *, $P < 0.05$; **, $P < 0.01$.

(Su *et al.*, 2011). Our analysis of previously published transcriptome data (de Marchi *et al.*, 2016) comparing gene expression in *ate1 ate2* with WT, and comparing gene expression during *Pst* infection in Col-0 and *ate1 ate2* also showed increased expression of RNAs encoding camalexin synthesis genes (Tables S3, S4). Analysis of transcript expression indicated greater accumulation for most genes of camalexin synthesis in mature uninfected leaves of *ntaq1* and *prt6* compared to WT (Figs 4, S7), including *PAD3* (CYP71B15), that catalyzes the final two steps of camalexin synthesis. Interestingly, during a time course following infiltration with *Pst* DC3000, levels of camalexin-associated transcripts, including *GSTF6* and *PAD3*, as well as *GSTF7* increased in WT but to a lesser extent in mutant leaves (Figs 4, S7). Whilst basal levels of camalexin in uninfected leaves were similar in mutants and WT they increased to a greater degree in mutants than WT in response to infection (Fig. 4). Mutant plants showed greater basal levels of indole-3-carboxylic acid (I3CA), a compound synthesized during the defence response and a potential precursor of camalexin through the action of GH3.5 (Forcat *et al.*, 2010;

Wang *et al.*, 2012) that was also upregulated at the RNA level in uninfected leaves of *ntaq1-3* (Fig. 4). Camalexin synthesis is highly interconnected with other pathways of secondary metabolism, for example it has been reported that *vte2* and *cyp83a1*, mutants of key steps of tocopherol and aliphatic glucosinolate synthesis pathways respectively, show increased levels of camalexin (Sattler *et al.*, 2006; Liu *et al.*, 2016). *VTE2* and *CYP83A1* showed decreased expression in *ntaq1-3* and *prt6-1* in both basal and infected conditions (Figs 4, S8). Combination of a null *pad3* allele with *prt6-1* resulted in a loss of the *prt6* enhanced resistance to injected *Pst* DC3000 (Fig. 5).

The Arg/N-end rule pathway regulates an age-dependent primed state in uninfected plants

Previous work showed that hypoxia-associated genes are ectopically upregulated in *prt6* and *ate1 ate2* mutant seedlings (Gibbs *et al.*, 2011; Licausi, 2013). However, it was recently shown that this is age-dependent, that in mature mutant plants these genes

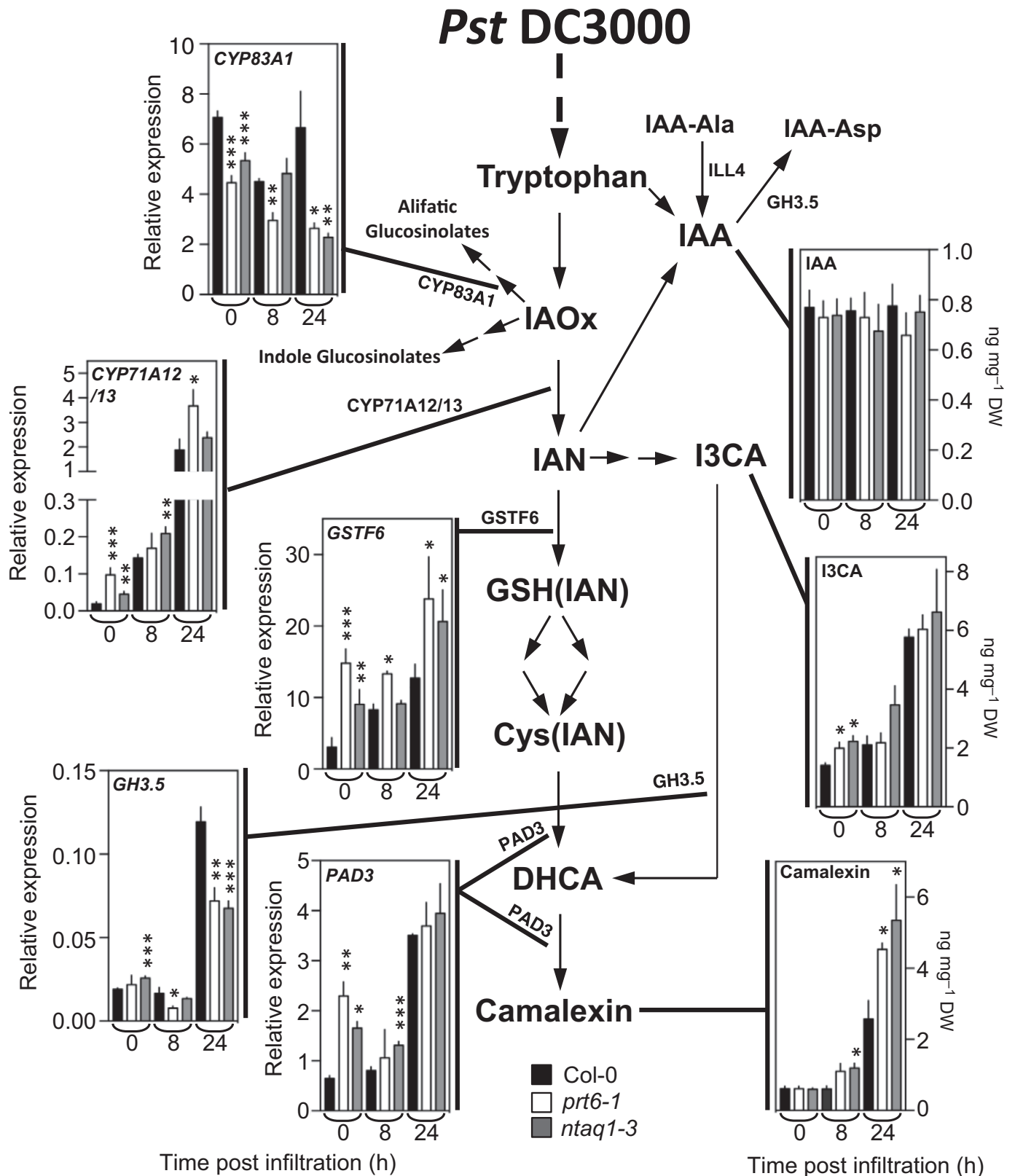


Fig. 4 Influence of NTAQ1 and PRT6 on camalexin and associated secondary metabolism in Arabidopsis in response to infiltration with *Pst* DC3000 (10^6 colony forming units (CFU) ml^{-1}). Schematic representation of the camalexin synthesis pathway highlighting time courses of changes in RNA expression (qRT-PCR) or metabolites in WT, *ntaq1-3* or *prt6-1* in response to bacterial infection. IAOx, indole-3-acetaldoxime; IAN, indole-3-acetonitrile; GSH, glutathione; DHCA, dihydrocamalexin acid; IAA, indole-3-acetic acid; I3CA, indole-3-carboxylic acid; GH3.5, IAA-AMIDO SYNTHASE; PAD3, PHYTOALEXIN DEFICIENT 3. Data represent means \pm SEM. Student's *t*-test: *, $P < 0.05$; **, $P < 0.01$; ***, $P < 0.001$.

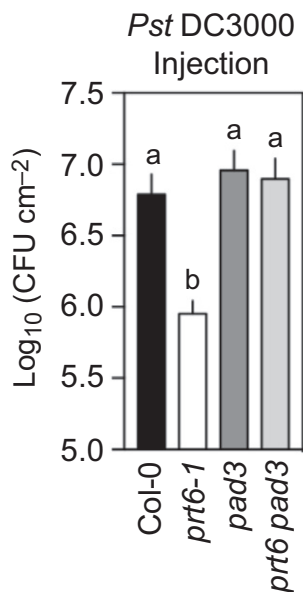


Fig. 5 Genetic interaction between *pad3* and *prt6* influences the Arabidopsis apoplastic response to *Pst* DC3000. Quantification of bacterial growth in wild type (WT) and mutant plants 4 d after bacterial infiltration (10^6 colony forming units (CFU) ml⁻¹). Data represent means \pm SEM. Statistical differences were analyzed by ANOVA followed by Tukey test ($P < 0.05$), significant differences indicated with letters.

are not upregulated (Giuntoli *et al.*, 2017). We also observe a large reduction in expression of hypoxia genes in older *prt6* plants and saw a similar trend in WT for some genes (Fig. S9a). No age-related differences were found in *NTAQ1* expression in either WT or *prt6* backgrounds (Fig. S9b), however *GSTF6/7* and *PAD3* showed increased expression with age in *prt6-1* and *ntaq1-3* plants compared with WT (Fig. 6a). In N-end rule mutants, compared to WT we found age-related increases for the SA-responsive PATHOGENESIS RELATED (PR) protein genes *PR1* and *PR5*, whilst JA and ET responsive *PR3* and *PR4* showed no differences (Fig. 6b). In barley, constitutive increase in expression of the SA-responsive genes *HvPR1* and *Hvβ1-3 glucanase* (Horvath *et al.*, 2003; Rostoks *et al.*, 2003) was found in leaves of *HvPRT6* RNAi plants, and infection with *Bgh* did not result in an increase in expression in *HvPRT6* RNAi plants, that was observed in WT plants (Fig. 6c).

Discussion

We show here that a role for Arg/N-end rule pathway-mediated immunity is conserved in flowering plants. In Arabidopsis we demonstrate physiological, biochemical and molecular roles for N-end rule component NTAQ1 in influencing basal defence by enhancing expression of defence proteins and synthesis of camalexin, and a role for the ERFVII known substrates in influencing stomatal response, against the hemibiotroph *Pst*. We show a role in barley of the Arg/N-end rule in response to the biotroph *Bgh* and hemibiotroph *Ps japonica*. We suggest that benefits of increased immunity may not be realized against necrotrophic pathogens (as shown in the interaction between *Fusarium* spp. and

barley). It has been documented that camalexin is part of the defence response against the necrotroph fungus *B. cinerea*, inhibiting its growth in a dose-dependent manner (Ferrari *et al.*, 2003). In our experiments, there were no differences in responses of WT and *prt6* to *B. cinerea* suggesting that independently of other mechanisms activated, an increase in camalexin in *prt6* may not reach a level necessary for reduction in fungal growth. A recent report showed N-end rule mutants, including alleles of *prt6*, *ate1* *ate2* and *ntaq1* to be in general equal or more sensitive than WT Arabidopsis to a wide range of bacterial and fungal pathogens with diverse infection strategies and lifestyles (de Marchi *et al.*, 2016). Our results, in which plants were grown under either neutral days or under the short-day condition used by de Marchi *et al.* showed the opposite results (of increased resistance). Our results provide a consistent pattern across different levels of expression (including enhanced defence gene transcripts and increased levels of camalexin synthesis proteins in untreated plants, and consistent phenotypes between Arabidopsis and barley) that indicate a role for NTAQ1 substrates and ERFVII as components of the immune response that enhance resistance. Therefore, differences in observed phenotypes of N-end rule mutants in response to infection between our studies remain to be resolved.

A specific effect for ERFVII was observed in the stomatal response to *Pst*. ABA is an important component of stomatal response to pathogens (McLachlan *et al.*, 2014) and stabilized ERFVII enhance ABA sensitivity of stomata (Vicente *et al.*, 2017). We observed a large increase in stability of artificial Nt-Cys reporters in both Arabidopsis and barley. Stabilisation could be caused by shielding of the Nt, or a reduction of either NO or oxygen. We did not observe an increase in hypoxia-related gene expression (of *ADHI*) at the same time as GUS stabilization, however we did observe a decline in NR activity. Seemingly contradictory to this assertion is the well known burst of NO in response to *Pst* infection (Delledonne *et al.*, 1998). However, this burst occurs early following infection, well before the reduction in NR activity and stabilization of artificial Nt-Cys reporters in both Arabidopsis and barley. It has previously been shown that in the NR null mutant *nia1 nia2*, which produces very low NO levels, the NO burst in response to infection is highly reduced (Modolo *et al.*, 2006; Chen *et al.*, 2014). Further experiments would be required to determine a causative role of reduced NR activity leading to enhanced stabilization. Regardless of the mechanism of stabilization, the observation of increased stability of Nt-Cys substrates following infection in both Arabidopsis and barley indicates a conserved role for modulation of the Cys-Arg/N-end rule pathway, and function for Nt-Cys substrates, in response to pathogen infection that deserves further investigation. Enhanced ABA sensitivity and stomatal response to *Pst* of the *ntaq1* mutant also suggests that Nt-Gln substrate(s) contribute to the stomatal ABA response to pathogens, and explains why *erfVII* is more sensitive to *Pst* than *prt6 erfVII* (where NTAQ1 substrates are still stabilized). An opposite effect of ERFVII was shown for interactions of Arabidopsis with the biotroph *P. brassicae*, as ERFVII enhanced infection indirectly by influencing fermentation (Gravot *et al.*, 2016).

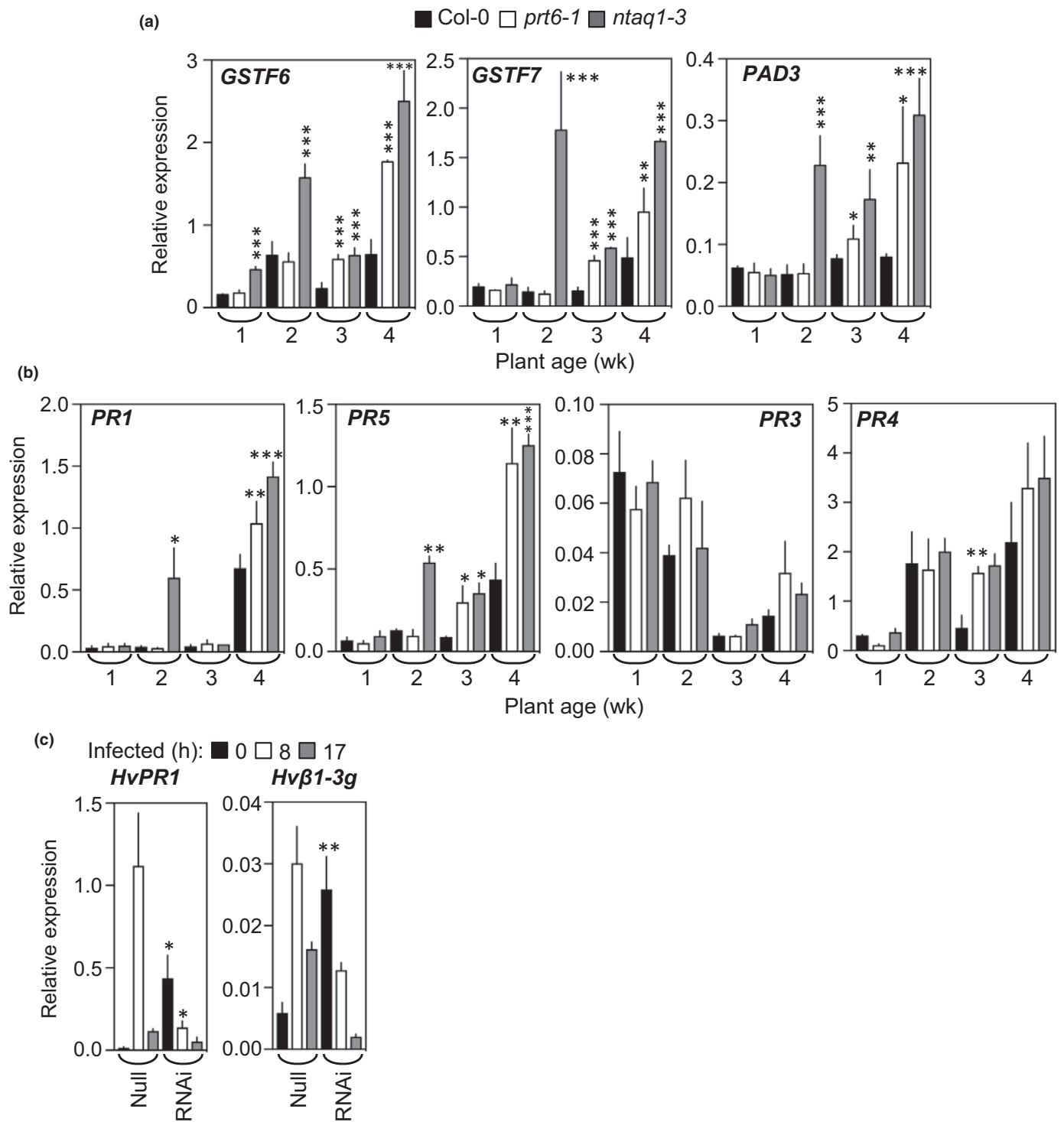


Fig. 6 Age-dependent priming of transcriptomic changes during *Arabidopsis* development and defence. (a) Relative expression of genes of camalexin synthesis in wild type (WT) and mutant plants. (b) Relative expression of transcripts encoding defence-related genes in WT and mutant plants. (c) Relative expression of *HvPR1* and *Hvβ1-3g* glucanase in WT and *HvPRT6* RNAi barley plants infected with *Blumeria graminis* f. sp. *hordei*. Data represent means \pm SEM. Statistical differences were analyzed by Student's *t*-test. *, $P < 0.05$; **, $P < 0.01$; ***, $P < 0.001$.

These observations and others (Gibbs *et al.*, 2015) indicate an important role for ERFVIIIs in the plant immune response.

Analysis of the response to *Pst* DC3000 *hrpA*⁻, together with increased expression of SA-associated defence genes and increased camalexin synthesis, suggests a role for NTAQ1 in the onset of

general and inducible PTI defence. An age-related increase in SA-related defence gene expression in N-end rule mutants was not matched by increased SA levels. This suggests a possible role for immune-related MAPK cascade activating MPK3/6 that are sufficient for SA-independent induction of most SA-responsive

genes, including *PR1* (Asai *et al.*, 2002). Concomitantly, it has been demonstrated that both MPK3 and MPK6 activation trigger GSTF6, 7 (and DJ1E) protein accumulation, which produces an increase in camalexin (Xu *et al.*, 2008; Su *et al.*, 2011). The observed increased accumulation of camalexin in *ntaq1* and *prt6* provides one explanation for the increased resistance of these mutants. Although expression of camalexin synthesis genes was ectopically upregulated in uninfected mature leaves of mutants, enhanced camalexin accumulation was only observed in response to infection. This may be the result of shunting of intermediate(s) to other secondary metabolism pathways. In line with this, unchallenged *ntaq1* and *prt6* plants show greater levels of I3CA. The observation that mutation of *pad3* reverts the enhanced resistance of *prt6* highlights the role of N-end rule regulated camalexin synthesis in enhancing the immune response.

How might NTAQ1 function during development and in response to pathogen attack? *NTAQ1* and *PRT6* expression do not change in response to pathogen attack. NTAQ1 function influences defence gene expression and camalexin synthesis. We demonstrate that downstream responses to NTAQ1, measured as responsive gene expression, are modified during development (although the expression of *NTAQ1* (and *PRT6*) transcripts were not affected by ageing), suggesting that NTAQ1 substrate(s) may show an age-dependent increase in abundance. Following protease cleavage their activity would be revealed in the *ntaq1* mutant, where they would remain ectopically stabilized. Following protease cleavage to reveal Nt-Gln, NTAQ1 substrates should be degraded in WT plants. In this case, in mature WT leaves down-regulation of NTAQ1-linked protease activity (or NTAQ1 activity) in response to pathogen attack could result in substrate stabilization. Stabilized NTAQ1 substrate(s) (or uncleaved protease targets that provide substrates) may then function to enhance gene expression associated with defence genes and camalexin synthesis, both resulting in an enhanced basal immune response.

Our data support a conserved role of the Arg/N-end rule pathway in influencing plant immune responses. Barley contains one *NTAQ1* gene (MLOC_70886) (Mayer *et al.*, 2012). Manipulation of expression or activity of this gene will be required to understand whether NTAQ1 activity is also required for defence in barley. An important goal of future work will be to identify Nt-Gln substrates that influence the immune response. Although NTAQ1-related genes are present in all major groups of eukaryotes, only a single example exists of a biochemical role for this enzyme and its associated substrate (*Usp1*) (Piatkov *et al.*, 2012). There is already evidence for Nt-Gln-bearing peptide fragments derived from proteins of diverse functions present in the plant METACASPASE-9 degradome (Tsiatsiani *et al.*, 2013), suggesting that substrates for NTAQ1 exist. Our results establish new components of the plant immune response, and offer new targets to enhance resistance against plant pathogens.

Acknowledgements

We thank Yin Yang and Daniel Beech (Nottingham) and Nancy De Winne (VIB, Gent) for technical assistance. This work was

supported by the Biotechnology and Biological Sciences Research Council (grant nos. BB/K000144/1, BB/M029441/1, BB/K000063/1) (all including financial support from SABMiller plc), D.R. by a BBSRC DTP PhD fellowship, G.M.M. by a Barry Axcell Fellowship, N.D. by a grants of the *ScienceCampus Halle – Plant-based Bioeconomy* for setting up a junior research group, the Leibniz Association, and the Leibniz Institute of Plant Biochemistry (IPB); C.N. by a PhD fellowship of the Landesgraduiertenförderung Sachsen-Anhalt and the Deutsche Forschungsgemeinschaft (DFG) Graduate Training Center GRK1026 ‘*Conformational Transitions in Macromolecular Interactions*’, C.C. and Y.I. were supported by Spanish Ministry of Economy and Competitiveness grant BIO2015-68130. Work in A.B.’s laboratory was supported by the ERA-Caps project N-vironment (Austrian Science Fund I1464-B16). V.P. was supported by Pla de formació Universitat Jaume I PI-1B2015-33 and the Instrumental Service of the University Jaume I SCIC.

Author contributions

J.V., G.M.M., K.S., C.N., N.D., D.J.G., R.V.R., C.C., A.B., J.E.G., K.G., M.J.H. designed research; J.V., G.M.M., J.P., V.P., Y.I., C.N., D.R., M.M., R.V.R., A.B. performed research; J.V., G.M.M., R.V.R., N.D., C.C., M.J.H. analyzed data; J.V. and M.J.H. wrote the manuscript.

ORCID

Nico Dissmeyer  <http://orcid.org/0000-0002-4156-3761>
Michael J. Holdsworth  <http://orcid.org/0000-0002-3954-9215>

References

- Abbas M, Berckhan S, Rooney DJ, Gibbs DJ, Conde JV, Correia CS, Bassel GW, Marin-de la Rosa N, Leon J, Alabadi D *et al.* 2015. Oxygen sensing coordinates photomorphogenesis to facilitate seedling survival. *Current Biology* 25: 1483–1488.
- Ajigboye OO, Bousquet L, Murchie EH, Ray RV. 2016. Chlorophyll fluorescence parameters allow the rapid detection and differentiation of plant responses in three different wheat pathosystems. *Functional Plant Biology* 43: 356–369.
- Arnaud D, Hwang I. 2015. A sophisticated network of signaling pathways regulates stomatal defenses to bacterial pathogens. *Molecular Plant* 8: 566–581.
- Asai T, Tena G, Plotnikova J, Willmann MR, Chiu WL, Gomez-Gomez L, Boller T, Ausubel FM, Sheen J. 2002. MAP kinase signalling cascade in *Arabidopsis* innate immunity. *Nature* 415: 977–983.
- Boller T, Felix G. 2009. A renaissance of elicitors: perception of microbe-associated molecular patterns and danger signals by pattern-recognition receptors. *Annual Review of Plant Biology* 60: 379–406.
- Chater C, Kamisugi Y, Movahedi M, Fleming A, Cuming AC, Gray JE, Beerling DJ. 2011. Regulatory mechanism controlling stomatal behavior conserved across 400 million years of land plant evolution. *Current Biology* 21: 1025–1029.
- Chen J, Vandelle E, Bellin D, Delle Donne M. 2014. Detection and function of nitric oxide during the hypersensitive response in *Arabidopsis thaliana*: where there’s a will there’s a way. *Nitric Oxide* 43: 81–88.

- Clough SJ, Bent AF. 1998. Floral dip: a simplified method for *Agrobacterium*-mediated transformation of *Arabidopsis thaliana*. *Plant Journal* 16: 735–743.
- Dangl JL, Jones JD. 2001. Plant pathogens and integrated defence responses to infection. *Nature* 411: 826–833.
- Davies RT, Goetz DH, Lasswell J, Anderson MN, Bartel B. 1999. IAR3 encodes an auxin conjugate hydrolase from *Arabidopsis*. *Plant Cell* 11: 365–376.
- Delledonne M, Xia Y, Dixon RA, Lamb C. 1998. Nitric oxide functions as a signal in plant disease resistance. *Nature* 394: 585–588.
- Dey S, Wenig M, Langen G, Sharma S, Kugler KG, Knappe C, Hause B, Bichlmeier M, Babaeizad V, Imani J *et al.* 2014. Bacteria-triggered systemic immunity in barley is associated with WRKY and ETHYLENE RESPONSIVE FACTORS but not with salicylic acid. *Plant Physiology* 166: 2133–2151.
- Ferrari S, Plotnikova JM, De Lorenzo G, Ausubel FM. 2003. *Arabidopsis* local resistance to *Botrytis cinerea* involves salicylic acid and camalexin and requires EDS4 and PAD2, but not SID2, EDS5 or PAD4. *Plant Journal* 35: 193–205.
- Forcat S, Bennett M, Grant M, Mansfield JW. 2010. Rapid linkage of indole carboxylic acid to the plant cell wall identified as a component of basal defence in *Arabidopsis* against *hnp* mutant bacteria. *Phytochemistry* 71: 870–876.
- Gamir J, Pastor V, Cerezo M, Flors V. 2012. Identification of indole-3-carboxylic acid as mediator of priming against *Plectosphaerella cucumerina*. *Plant Physiology and Biochemistry* 61: 169–179.
- Gibbs DJ, Bacardit J, Bachmair A, Holdsworth MJ. 2014a. The eukaryotic N-end rule pathway: conserved mechanisms and diverse functions. *Trends in Cell Biology* 24: 603–611.
- Gibbs DJ, Conde JV, Berckhan S, Prasad G, Mendiondo GM, Holdsworth MJ. 2015. Group VII Ethylene Response Factors coordinate oxygen and nitric oxide signal transduction and stress responses in plants. *Plant Physiology* 169: 23–31.
- Gibbs DJ, Isa NM, Movahedi M, Lozano-Juste J, Mendiondo GM, Berckhan S, Marin-de la Rosa N, Conde JV, Correia CS, Pearce SP *et al.* 2014b. Nitric oxide sensing in plants is mediated by proteolytic control of Group VII ERF transcription factors. *Molecular Cell* 53: 369–379.
- Gibbs DJ, Lee SC, Isa NM, Gramuglia S, Fukao T, Bassel GW, Sousa Correia C, Corbineau F, Theodoulou FL, Bailey-Serres J *et al.* 2011. Homeostatic response to hypoxia is regulated by the N-end rule pathway in plants. *Nature* 479: 415–418.
- Giuntoli B, Shukla V, Maggiorelli F, Giorgi FM, Lombardi L, Perata P, Licausi F. 2017. Age-dependent regulation of ERF-VII transcription factor activity in *Arabidopsis thaliana*. *Plant, Cell & Environment* 40: 2333–2346.
- Glazebrook J, Ausubel FM. 1994. Isolation of phytoalexin-deficient mutants of *Arabidopsis thaliana* and characterization of their interactions with bacterial pathogens. *Proceedings of the National Academy of Sciences, USA* 91: 8955–8959.
- Graciet E, Mesiti F, Wellmer F. 2010. Structure and evolutionary conservation of the plant N-end rule pathway. *Plant Journal* 61: 741–751.
- Grant MR, Jones JDG. 2009. Hormone (Dis)harmony moulds plant health and disease. *Science* 324: 750–752.
- Gravot A, Richard G, Lime T, Lemarié S, Jubault M, Lariagon C, Lemoine J, Vicente J, Robert-Seilaniantz A, Holdsworth MJ *et al.* 2016. Hypoxia response in *Arabidopsis* roots infected by *Plasmidiophora brassicae* supports the development of clubroot. *Bmc Plant Biology* 16: 251.
- Grigoryev S, Stewart AE, Kwon YT, Arfin SM, Bradshaw RA, Jenkins NA, Copeland NG, Varshavsky A. 1996. A mouse amidase specific for N-terminal asparagine – the gene, the enzyme, and their function in the N-end rule pathway. *Journal of Biological Chemistry* 271: 28521–28532.
- Horvath H, Rostoks N, Brueggeman R, Steffenson B, von Wettstein D, Kleinohfs A. 2003. Genetically engineered stem rust resistance in barley using the *Rpg1* gene. *Proceedings of the National Academy of Sciences, USA* 100: 364–369.
- Hu RG, Sheng J, Qi X, Xu ZM, Takahashi TT, Varshavsky A. 2005. The N-end rule pathway as a nitric oxide sensor controlling the levels of multiple regulators. *Nature* 437: 981–986.
- Kaiser JJ, Lewis OAM. 1984. Nitrate reductase and glutamine-synthetase activity in leaves and roots of nitrate-fed *Helianthus-annuus* L. *Plant and Soil* 77: 127–130.
- Karimi M, Bleys A, Vanderhaeghen R, Hilson P. 2007. Building blocks for plant gene assembly. *Plant Physiology* 145: 1183–1191.
- Lehmeyer M, Kanofsky K, Hanko EK, Ahrendt S, Wehrs M, Machens F, Hehl R. 2016. Functional dissection of a strong and specific microbe-associated molecular pattern-responsive synthetic promoter. *Plant Biotechnology Journal* 14: 61–71.
- Licausi F. 2013. Molecular elements of low-oxygen signaling in plants. *Physiologia Plantarum* 148: 1–8.
- Licausi F, Kosmacz M, Weits DA, Giuntoli B, Giorgi FM, Voeselek LACJ, Perata P, van Dongen JT. 2011. Oxygen sensing in plants is mediated by an N-end rule pathway for protein destabilization. *Nature* 479: 419–422.
- Liu S, Bartnikas LM, Volko SM, Ausubel FM, Tang D. 2016. Mutation of the glucosinolate biosynthesis enzyme cytochrome P450 83A1 monooxygenase increases camalexin accumulation and powdery mildew resistance. *Frontiers in Plant Science* 7: 227.
- de Marchi R, Sorel M, Mooney B, Fudal I, Goslin K, Kwasińska K, Ryan PT, Pfalz M, Kroymann J, Pollmann S *et al.* 2016. The N-end rule pathway regulates pathogen responses in plants. *Scientific Reports* 6: 26020.
- Mayer KFX, Waugh R, Langridge P, Close TJ, Wise RP, Graner A, Matsumoto T, Sato K, Schulman A, Muehlbauer GJ *et al.* 2012. A physical, genetic and functional sequence assembly of the barley genome. *Nature* 491: 711–716.
- McAinsh MR, Brownlee C, Hetherington AM. 1991. Partial inhibition of ABA-induced stomatal closure by calcium-channel blockers. *Proceedings of the Royal Society B: Biological Sciences* 243: 195–201.
- McLachlan DH, Kopischke M, Robatzek S. 2014. Gate control: guard cell regulation by microbial stress. *New Phytologist* 203: 1049–1063.
- Mendiondo GM, Gibbs DJ, Szurman-Zubrzycka M, Korn A, Marquez J, Szarejko I, Maluszynski M, King J, Axcell B, Smart K *et al.* 2016. Enhanced waterlogging tolerance in barley by manipulation of expression of the N-end rule pathway E3 ligase PROTEOLYSIS6. *Plant Biotechnology Journal* 14: 40–50.
- Modolo LV, Augusto O, Almeida IMG, Pinto-Maglio CAF, Oliveira HC, Seligman K, Salgado I. 2006. Decreased arginine and nitrite levels in nitrate reductase-deficient *Arabidopsis thaliana* plants impair nitric oxide synthesis and the hypersensitive response to *Pseudomonas syringae*. *Plant Science* 171: 34–40.
- Moreno JJ, Martin R, Castresana C. 2005. *Arabidopsis* SHMT1, a serine hydroxymethyltransferase that functions in the photorespiratory pathway influences resistance to biotic and abiotic stress. *Plant Journal* 41: 451–463.
- Nawrath C, Metraux JP. 1999. Salicylic acid induction-deficient mutants of *Arabidopsis* express PR-2 and PR-5 and accumulate high levels of camalexin after pathogen inoculation. *Plant Cell* 11: 1393–1404.
- Park BS, Song JT, Seo HS. 2011. *Arabidopsis* nitrate reductase activity is stimulated by the E3 SUMO ligase AtSIZ1. *Nature Communications* 2: 400.
- Piatkov KI, Colnaghi L, Bekes M, Varshavsky A, Huang TT. 2012. The auto-generated fragment of the Usp1 deubiquitylase is a physiological substrate of the N-end rule pathway. *Molecular Cell* 48: 926–933.
- Piatkov KI, Oh JH, Liu Y, Varshavsky A. 2014. Calpain-generated natural protein fragments as short-lived substrates of the N-end rule pathway. *Proceedings of the National Academy of Sciences, USA* 111: E817–E826.
- Pieterse CMJ, Leon-Reyes A, Van der Ent S, Van Wees SCM. 2009. Networking by small-molecule hormones in plant immunity. *Nature Chemical Biology* 5: 308–316.
- Rostoks N, Schmierer D, Kudrna D, Kleinohfs A. 2003. Barley putative hypersensitive induced reaction genes: genetic mapping, sequence analyses and differential expression in disease lesion mimic mutants. *Theoretical and Applied Genetics* 107: 1094–1101.
- Sánchez-Bel P, Sanmartín N, Pastor V, Mateu D, Cerezo M, Vidal-Albalat A, Pastor-Fernández J, Pozo MJ, Flors V. 2018. Mycorrhizal tomato plants fine tunes the growth-defence balance upon N depleted root environments. *Plant, Cell & Environment* 41: 406–420.
- Sappl PG, Carroll AJ, Clifton R, Lister R, Whelan J, Millar AH, Singh KB. 2009. The *Arabidopsis* glutathione transferase gene family displays complex stress regulation and co-silencing multiple genes results in altered metabolic sensitivity to oxidative stress. *Plant Journal* 58: 53–68.
- Sattler SE, Mene-Saffrane L, Farmer EE, Krischke M, Mueller MJ, DellaPenna D. 2006. Nonenzymatic lipid peroxidation reprograms gene expression and activates defense markers in *Arabidopsis* tocopherol-deficient mutants. *Plant Cell* 18: 3706–3720.

- Schilling S, Stenzel I, von Bohlen A, Wermann M, Schulz K, Demuth HU, Wasternack C. 2007. Isolation and characterization of the glutaminyl cyclases from *Solanum tuberosum* and *Arabidopsis thaliana*: implications for physiological functions. *Biological Chemistry* **388**: 145–153.
- Su T, Xu J, Li Y, Lei L, Zhao L, Yang H, Feng J, Liu G, Ren D. 2011. Glutathione-indole-3-acetonitrile is required for camalexin biosynthesis in *Arabidopsis thaliana*. *Plant Cell* **23**: 364–380.
- Thao S, Zhao Q, Kimball T, Steffen E, Blommel PG, Ritters M, Newman CS, Fox BG, Wrobel RL. 2005. Results from high-throughput DNA cloning of *Arabidopsis thaliana* target genes using site-specific recombination. *Journal of Structural and Functional Genomics* **5**: 267–276.
- Thordal-Christensen H, Zhang ZG, Wei YD, Collinge DB. 1997. Subcellular localization of H₂O₂ in plants. H₂O₂ accumulation in papillae and hypersensitive response during the barley–powdery mildew interaction. *Plant Journal* **11**: 1187–1194.
- Truman W, de Zabala MT, Grant M. 2006. Type III effectors orchestrate a complex interplay between transcriptional networks to modify basal defence responses during pathogenesis and resistance. *Plant Journal* **46**: 14–33.
- Tsiatsiani L, Timmerman E, De Bock P-J, Vercammen D, Stael S, van de Cotte B, Staes A, Goethals M, Beunens T, Van Damme P *et al.* 2013. The Arabidopsis METACASPASE9 degradome. *Plant Cell* **25**: 2831–2847.
- Varshavsky A. 2012. The ubiquitin system, an immense realm. *Annual Review of Biochemistry* **81**: 167–176.
- Vicente J, Mendiondo GM, Movahedi M, Peirats-Llobet M, Juan YT, Shen YY, Dambire C, Smart K, Rodriguez PL, Charny YY *et al.* 2017. The Cys-Arg/N-end rule pathway is a general sensor of abiotic stress in flowering plants. *Current Biology* **27**: 3183–3190.
- Vu LD, Stes E, Van Bel M, Nelissen H, Maddelein D, Inze D, Coppens F, Martens L, Gevaert K, De Smet I. 2016. Up-to-date workflow for plant (phospho)proteomics identifies differential drought-responsive phosphorylation events in maize leaves. *Journal of Proteome Research* **15**: 4304–4317.
- Wang HQ, Piatkov KI, Brower CS, Varshavsky A. 2009. Glutamine-specific N-terminal amidase, a component of the N-end rule pathway. *Molecular Cell* **34**: 686–695.
- Wang MY, Liu XT, Chen Y, Xu XJ, Yu B, Zhang SQ, Li Q, He ZH. 2012. Arabidopsis acetyl-amido synthetase GH3.5 involvement in camalexin biosynthesis through conjugation of indole-3-carboxylic acid and cysteine and upregulation of camalexin biosynthesis genes. *Journal of Integrative Plant Biology* **54**: 471–485.
- Weits DA, Giuntoli B, Kosmacz M, Parlanti S, Hubberten HM, Riegler H, Hoefgen R, Perata P, van Dongen JT, Licausi F. 2014. Plant cysteine oxidases control the oxygen-dependent branch of the N-end-rule pathway. *Nature Communications* **5**: 3425.
- White MD, Klecker M, Hopkinson RJ, Weits DA, Mueller C, Naumann C, O'Neill R, Wickens J, Yang JY, Brooks-Bartlett JC *et al.* 2017. Plant cysteine oxidases are dioxygenases that directly enable arginyl transferase-catalysed arginylation of N-end rule targets. *Nature Communications* **8**: 14690.
- Xu F, Huang Y, Li L, Gannon P, Linster E, Huber M, Kapos P, Bienvenut W, Plevoda B, Meinel T *et al.* 2015. Two N-terminal acetyltransferases antagonistically regulate the stability of a Nod-like receptor in Arabidopsis. *Plant Cell* **27**: 1547–1562.
- Xu J, Li Y, Wang Y, Liu H, Lei L, Yang H, Liu G, Ren D. 2008. Activation of MAPK kinase 9 induces ethylene and camalexin biosynthesis and enhances sensitivity to salt stress in Arabidopsis. *Journal of Biological Chemistry* **283**: 26996–27006.
- Zhao J, Last RL. 1996. Coordinate regulation of the tryptophan biosynthetic pathway and indolic phytoalexin accumulation in Arabidopsis. *Plant Cell* **8**: 2235–2244.
- Zhou BJ, Zeng LR. 2017. Conventional and unconventional ubiquitination in plant immunity. *Molecular Plant Pathology* **18**: 1313–1330.

Supporting Information

Additional Supporting Information may be found online in the Supporting Information section at the end of the article:

Fig. S1 Identification of Arabidopsis *ntaq1* alleles.

Fig. S2 Influence of N-end rule mutants on bacterial growth.

Fig. S3 Influence of N-end rule mutants on pathogen growth.

Fig. S4 Quantification of RNA expression.

Fig. S5 Influence of N-end rule mutants on oxidative response to infection by *Pst*.

Fig. S6 Time course quantification of phytohormone levels in response to *Pst* DC3000 infiltration of mature leaves in *ntaq1*, *prt6* and WT.

Fig. S7 Quantification of RNA expression during infection with *Pst*.

Fig. S8 Quantification of RNA expression in response to *Pst* DC3000 infiltration of mature leaves of *VTE2* (a key gene for tocopherols biosynthesis) during *Pst* DC3000 infection following infiltration.

Fig. S9 Age-related changes in gene expression.

Table S1 Oligonucleotide primer sequences used for qRT-PCT, RT-PCR and genotyping

Table S2 Shotgun proteome analysis comparing Col-0 (WT) and *ntaq1-3*

Table S3 Expression of proteins identified as upregulate in *ntaq1* compared with WT in datasets provided by de Marchi *et al.* (2016)

Table S4 Expression of genes of camalexin synthesis and associated pathways in datasets provided by de Marchi *et al.* (2016)

Please note: Wiley Blackwell are not responsible for the content or functionality of any Supporting Information supplied by the authors. Any queries (other than missing material) should be directed to the *New Phytologist* Central Office.